General Theory of Static Response for Markov Jump Processes

Timur Aslyamov[*] and Massimiliano Esposito[†]

Department of Physics and Materials Science, University of Luxembourg, L-1511 Luxembourg City, Luxembourg

We consider Markov jump processes on a graph described by a rate matrix that depends on various control parameters. We derive explicit expressions for the static responses of edge currents and steady-state probabilities. We show that they are constrained by the graph topology (i.e., the incidence matrix) by deriving response relations (i.e., linear constraints linking the different responses) and topology-dependent bounds. For unicyclic networks, all scaled current responses are between zero and one and must sum to one. Applying these results to stochastic thermodynamics, we derive explicit expressions for the static response of fundamental currents (which carry the full dissipation) to fundamental thermodynamic forces (which drive the system away from equilibrium).

Introduction—Nonequilibrium steady state (NESS) of Markov jump processes describe a plethora of phenomena [1] and understanding their response to external perturbations has crucial implications [2] across fields, such as biology [3–6], nanoelectronics [7,8], and deep learning [9]. When the Markov jump process is produced by thermal noise, near equilibrium, the response is simple and characterized by the dissipation-fluctuation relation (DFR) [10,11]. But far-from-equilibrium or for nonthermal processes, the response is significantly more involved; see Refs. [12–24]. Recently, for the static response, exact results [25–27] and tight bounds [28,29] have been derived assuming Arrhenius-like rates. Moreover, the bounds [25] only hold for local responses, i.e., when the perturbation and the observable are assigned to the same transition.

In this Letter, we build a general static response theory for any Markov jump processes, which describes both local and nonlocal responses for arbitrary parameterizations of the rate matrix. We identify a broad class of parametrizations that produce two types of linear constraints, which we call the summation response relation (SRR) and cycle response relation (CRR). The SRR restricts the responses of the edge flux and probability. The form of such constraints does not depend on the topology of the incidence matrix, but the values of the responses involved strongly depend on it. The CRR limits the sum of local responses by the number of fundamental (Schnakenberg [30]) cycles, which are essential topological characteristics. Moreover, the topology defines which static responses among all combinatorial configurations have universal (remarkably simple) bounds. In unicyclic networks, all responses are bounded; for multicyclic systems, our approach identifies bounded and

unbounded responses. In concrete examples considered, the sizes of bounded and unbounded sets are comparable. Finally, for Markov jump processes describing a system in contact with thermal reservoirs (i.e., stochastic thermodynamics), we derive an explicit expression for the static response of fundamental currents to fundamental thermodynamic forces. The former characterize the full dissipation and the latter drive the system out of equilibrium.

Setup—We consider a directed graph $\mathcal{G}$ with N nodes and N_e edges and a Markov jump process over the discrete set $\mathcal{S}$ of the N states corresponding to the nodes. Then, the edges $e \in \mathcal{E}$ of $\mathcal{G}$ define possible transitions with the probability rates encoded in the rate matrix $\mathbb{W}/\tau$. In this description, the jump from n to m is the edge (arrow) $+e$ with the source $s(+e) = n$ and the tip $t(+e) = m$. For the reverse transition, we have $-e$ with $s(-e) = m$ and $t(-e) = n$. Choosing $\tau = 1$ the nondiagonal elements $W_{nm} = W_e \geq 0$ become the probabilities per unit of time assigned to the edges e. We assume that the matrix $\mathbb{W}$ is irreducible [31] and that all transitions are reversible, i.e., $W_e \neq 0$ only if $W_{-e} \neq 0$. With the property of diagonal elements $W_{ii} = -\sum_{j \neq i} W_{ij}$ the described system always exhibits a unique steady-state probability $\boldsymbol{\pi} = (\pi_1, \ldots, \pi_N)^{\mathsf{T}}$ that satisfies

$$\mathbb{W} \cdot \boldsymbol{\pi} = \mathbf{0}, \tag{1}$$

with the normalization $\sum_{i=1}^{N} \pi_i = 1$. We define the transition current along the edge e as $j_e \equiv W_{+e}\pi_{s(+e)} - W_{-e}\pi_{s(-e)}$. This definition has a matrix form $\boldsymbol{j} = \mathbb{\Gamma}\boldsymbol{\pi}$, where the matrix $\mathbb{\Gamma}$ has elements $\Gamma_{ei} \equiv W_{+e}\delta_{is(+e)} - W_{-e}\delta_{is(-e)}$ with the Kronecker symbol δ. In analogy to linear chemical reaction networks [32–34], the rate matrix can be decomposed as $\mathbb{W} = \mathbb{S}\mathbb{\Gamma}$, where $\mathbb{S}$ is the incidence matrix of the directed graph $\mathcal{G}$ with the elements $S_{ie} \equiv \delta_{is(-e)} - \delta_{is(+e)}$.

[*]Contact author: timur.aslyamov@uni.lu
[†]Contact author: massimiliano.esposito@uni.lu

We introduce a parametrization $\mathbb{W}(\boldsymbol{p})$ using the vector $\boldsymbol{p} = (\dots, p, \dots)^{\intercal}$ made of N_p control parameters $p \in \boldsymbol{p}$. Thus, the steady-state condition (1) can be written as

$$\mathbb{S} \cdot \boldsymbol{j}(\boldsymbol{p}) = \boldsymbol{0}, \tag{2}$$

where $\boldsymbol{j}(\boldsymbol{p}) \equiv \boldsymbol{j}[\boldsymbol{p}, \boldsymbol{\pi}(\boldsymbol{p})]$ depends on $\boldsymbol{p}$ both explicitly due to $\Gamma(\boldsymbol{p})$ and implicitly due to $\boldsymbol{\pi}(\boldsymbol{p})$. The central objects of this work are the static responses of a quantity $q(\boldsymbol{p})$ (e.g., a probability $\boldsymbol{\pi}$ or a current $\boldsymbol{j}$) to perturbations of the parameters p, i.e., the elements of the vector $\nabla_{\boldsymbol{p}} q(\boldsymbol{p}) = (\dots, d_p q, \dots)^{\intercal}$. Our goal will be to obtain *explicit* relations for these responses enabling us to find relations among them. Many recent works considered edge perturbations where each element of $\boldsymbol{p}$ acts on a rate associated with a given edge [25–27,35,36]. But often, perturbing physical quantities implies acting on rates associated with many edges. In this Letter, after an example, we go from generic perturbations to more specific ones, illustrating our findings at every stage using a physical model.

Homogeneous parametrization—We first provide a simple illustration of how a given parametrization can give rise to nontrivial relations among static responses: let us consider the parametrization $\boldsymbol{h} = (\dots, h_p, \dots)^{\intercal}$ of $\mathbb{W}(\boldsymbol{h})$ such that

$$\mathbb{W}(\alpha \boldsymbol{h}) = \alpha^k \mathbb{W}(\boldsymbol{h}), \tag{3}$$

where k is the positive order of the homogeneous function. The fact that $\mathbb{W}(\alpha \boldsymbol{h}) \boldsymbol{\pi}(\alpha \boldsymbol{h}) = \alpha^k \mathbb{W}(\boldsymbol{h}) \boldsymbol{\pi}(\alpha \boldsymbol{h}) = 0$ implies that $\boldsymbol{\pi}(\boldsymbol{h}) = \boldsymbol{\pi}(\alpha \boldsymbol{h})$ since the solution of Eq. (1) is unique; $\boldsymbol{\pi}(\boldsymbol{h})$ is therefore an homogeneous function of order zero of $\boldsymbol{h}$ which implies the linear relation (Euler's theorem for $k = 0$)

$$\sum_p h_p \frac{d\boldsymbol{\pi}}{dh_p} = 0. \tag{4}$$

This in turn implies that the current is a homogeneous function $\boldsymbol{j}[\alpha \boldsymbol{h}, \boldsymbol{\pi}(\alpha \boldsymbol{h})] = \alpha^k \boldsymbol{j}[\boldsymbol{h}, \boldsymbol{\pi}(\boldsymbol{h})]$, which is equivalent to

$$\sum_p h_p \frac{d\boldsymbol{j}}{dh_p} = k\boldsymbol{j}. \tag{5}$$

Equations (4) and (5) are known in metabolic control analysis as summation theorems [37–40]. In that context, enzyme concentrations play the role of the homogeneous parameters.

Matrix approach to static response—We now turn to arbitrary parametrizations. Our strategy is to use $\sum_{i=1}^{N} \pi_i = 1$, and thus $d_p \pi_N = -\sum_{k=1}^{N-1} d_p \pi_k$, to arrive at $N - 1$ independent equations for others $d_p \pi_k$ with $k \in \hat{\mathcal{S}} \equiv \mathcal{S} \backslash \{N\}$. To solve this linear problem, we introduce

the matrix $\mathbb{K} \equiv \hat{\mathbb{S}} \hat{\Gamma}$, where $\hat{\mathbb{S}} \equiv [S_{ke}]_{\{k,e\}}$ and $\hat{\Gamma} \equiv [\Gamma_{ek} - \Gamma_{eN}]_{\{e,k\}}$ are reduced matrices with $k \in \hat{\mathcal{S}}$ and $e \in \mathcal{E}$. In Sec. A of the Supplemental Material [41] we prove that the matrix $\mathbb{K}$ is invertible [see Eq. (A5)], and that the probability and current response matrices read

$$\mathbb{R}^{\pi} \equiv [d_p \pi_i]_{\{i,p\}} = - \begin{pmatrix} \mathbb{K}^{-1} \hat{\mathbb{S}} \mathbb{J} \\ -\sum_k (\mathbb{K}^{-1} \hat{\mathbb{S}} \mathbb{J})_k^{\intercal} \end{pmatrix}, \tag{6a}$$

$$\mathbb{R}^j \equiv [d_p j_e]_{\{e,p\}} = \mathbb{P} \mathbb{J}. \tag{6b}$$

Here, $\sum_k (\mathbb{K}^{-1} \hat{\mathbb{S}} \mathbb{J})_k^{\intercal}$ denotes the row that is the sum of all rows of the matrix $\mathbb{K}^{-1} \hat{\mathbb{S}} \mathbb{J}$; $\{i, p\}$ ($\{e, p\}$) denote the sets of indexes $i \in \mathcal{S}$ ($e \in \mathcal{E}$) for rows and $p \in \boldsymbol{p}$ for columns; $\mathbb{J} \equiv [\partial_p j_e]_{\{e,p\}}$ is the steady state Jacobian

$$\mathbb{J} = [\pi_{s(+e)} \partial_p W_e(\boldsymbol{p}) - \pi_{s(-e)} \partial_p W_{-e}(\boldsymbol{p})]_{\{e,p\}}, \tag{7}$$

and the matrix $\mathbb{P} = [P_{ee'}]_{\{e,e'\}}$ is defined as

$$\mathbb{P} \equiv \left[\delta_{ee'} - \sum_{x,x' \in \hat{\mathcal{S}}} \hat{\Gamma}_{ex} (\mathbb{K}^{-1})_{xx'} S_{x'e'} \right]_{\{e,e'\}} = \mathbb{I} - \hat{\Gamma}(\hat{\mathbb{S}} \hat{\Gamma})^{-1} \hat{\mathbb{S}}, \tag{8}$$

with $\mathbb{I}$ denoting the identity matrix. Matrix $\mathbb{P}$ is idempotent [$\mathbb{P}^2 = \mathbb{P}$] and is known as an oblique projection matrix [44]. Since $\hat{\mathbb{S}} \mathbb{P} = 0$, we define $\mathbb{B}$ via

$$\mathbb{P} \equiv \left[\sum_{\gamma \in \mathcal{C}} c_e^{\gamma} B_{\gamma e'} \right]_{\{e,e'\}} = \mathbb{C} \mathbb{B}, \tag{9}$$

where $\mathbb{C} = (\dots, \boldsymbol{c}_{\gamma}, \dots)$ is the matrix of the fundamental cycles $\boldsymbol{c}^{\gamma}$ defined as the right null vectors of the incidence matrix $\mathbb{S} \boldsymbol{c}^{\gamma} = \boldsymbol{0}$ ($\mathbb{S}$ and $\hat{\mathbb{S}}$ share the same N_c cycles). Equation (6) is crucial in what follows. It contains explicit expressions for the responses of all edges to arbitrary perturbations and contains information on how they are related to each other.

Response relations—For a vector $\boldsymbol{p}$ such that the matrix $\mathbb{J}$ in Eq. (7) is full row rank (rk$\mathbb{J} = N_e$, i.e., $N_p \geq N_e$), we can always find a right invertible matrix $\mathbb{J}^+$ such that $\mathbb{J} \mathbb{J}^+ = \mathbb{I}$:

$$\mathbb{J}^+ \equiv \mathbb{J}^{\intercal} (\mathbb{J} \mathbb{J}^{\intercal})^{-1}. \tag{10}$$

Multiplying both sides of Eqs. (6a) and (6b) by the vector $\mathbb{J}^+ \boldsymbol{j}$, we arrive at $\mathbb{R}^{\pi} \mathbb{J}^+ \boldsymbol{j} = \boldsymbol{0}$ and $\mathbb{R}^j \mathbb{J}^+ \boldsymbol{j} = \mathbb{P} \boldsymbol{j} = \mathbb{I} \boldsymbol{j}$. In coordinate form, these relations give rise to the SRRs:

$$\sum_{p \in \boldsymbol{p}} \phi_p d_p \pi_i = 0, \qquad \sum_{p \in \boldsymbol{p}} \phi_p d_p j_e = j_e, \tag{11}$$
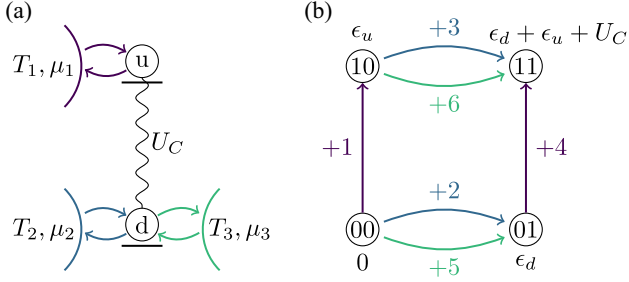
FIG. 1. (a) Double QDs u and d coupled with three reservoirs (purple, blue, green). The reservoirs have different temperatures T_i ($\beta_i = 1/T_i$) and chemical potentials μ_i, where $i = 1, 2, 3$. (b) Graph representation: Four states 00, 01, 10, and 11 have energies 0, ϵ_u, ϵ_d, and $\epsilon_d + \epsilon_u + U_C$, respectively, where U_C is the Coulomb repulsion energy arising when the two dots are filled. The colored arrows show the transitions assigned to the corresponding reservoir. The transition rates read $W_{\pm e} = \Gamma_e[1 + \exp(\pm\Psi_e)]^{-1}$, where Γ_e are the tunneling rates and Ψ_e are the edge parameters (the potential assigned to the transition $+e$): $\Psi_1 = \beta_1(\epsilon_u - \mu_1)$, $\Psi_2 = \beta_2(\epsilon_d - \mu_2)$, $\Psi_3 = \beta_2(\epsilon_d + U_C - \mu_2)$, $\Psi_4 = \beta_1(\epsilon_u + U_C - \mu_1)$, $\Psi_5 = \beta_3(\epsilon_d - \mu_3)$, and $\Psi_6 = \beta_3(\epsilon_d + U_C - \mu_3)$.

where ϕ_p are elements of the vector

$$\boldsymbol{\phi} \equiv \mathbb{J}^+ \cdot \boldsymbol{j}. \tag{12}$$

Equations (11) generalize Eq. (4) and (5) beyond homogeneous parameters with the only difference that the h_p's are now replaced by the coefficients ϕ_p. The structure of Eq. (11) is universal, and the parametrization as well as the topology of the graph are encoded only in the vector Eq. (12), which can be easily calculated explicitly using Eq. (7). The SRR for the current in Eq. (11) constrains the response of the edge fluxes. It implies that all flux responses of a given edge e vanish ($d_p j_e = 0$ for all $p \in \boldsymbol{p}$) only when that edge is at equilibrium, i.e., when $j_e = 0$.

Physical example: We consider the double quantum dots (QDs) model shown in Fig. 1(a) [45–48]. Each QD consists of a single electronic level with energy ϵ_u, (ϵ_d), that can be solid or empty due to electron exchanges with the reservoirs. Electrons cannot be transferred between the two QDs, but when the two QDs are occupied, they interact with each other via a Coulomb repulsion energy U_C. The four many-body states of the system and their corresponding energy are shown in Fig. 1(b). In this case, the general explicit expressions for responses, Eq. (6), hold for any parametrization. But to satisfy the SRRs, we must have at least 6 independent model parameters ($N_p \geq N_e = 6$ and $\mathbb{J}$ must be full row rank): The set $\{\epsilon_u, \epsilon_d, U_C\}$ is not large enough [Eq. (B2) in [41]], the set $\{\epsilon_u, \epsilon_d, U_C, \mu_1, \mu_2, \mu_3\}$ is not independent as $\det \mathbb{J} = 0$ [Eq. (B3) in [41]], but the set $\{\epsilon_u, \epsilon_d, U_C, \beta_1, \beta_2, \beta_3\}$ would work as $\det \mathbb{J} \neq 0$ [Eq. (B4) in [41]].

Independent edge perturbations—We now restrict our theory to systems with independent parameters at every edge, namely, $\mathrm{rk}\mathbb{J} = N_p = N_e$. In this case, every element p_e of the vector $\boldsymbol{p}$ is assigned to its own edge e, which implies that the matrix $\mathbb{J}(\boldsymbol{p}) = \mathrm{diag}(\ldots, \partial_{p_e} j_e, \ldots)$ is diagonal and $\mathbb{J}^+ = \mathbb{J}^{-1}$. Using Eq. (12), the coefficients ϕ_e take the explicit form

$$\phi_e = \left(\frac{\partial j_e}{\partial p_e}\right)^{-1} j_e. \tag{13}$$

Since the matrix $\mathbb{J}$ is diagonal, we can rewrite Eq. (6b) as

$$P_{ee'} = \left(\frac{\partial j_{e'}}{\partial p_{e'}}\right)^{-1} \frac{d j_e}{d p_{e'}}. \tag{14}$$

This shows that the elements $P_{ee'}$ are scaled responses where the scaling factor $\partial_{p_{e'}} j_{e'}$ is controlled by the explicit dependence $W_{\pm e}(\boldsymbol{p})$ and can be interpreted as the instantaneous response, as the edge probabilities $\pi_{s(\pm e')}$ had no time to change. This means that $P_{ee'}$ can be seen as the ratio between the complete and instantaneous response.

Physical example: For the QDs of Fig. 1, edge perturbation can be realized using the set $\boldsymbol{\Gamma} = (\ldots, \Gamma_e, \ldots)^\mathsf{T}$. The set $\{\epsilon_u, \epsilon_d, U_C, \beta_1, \beta_2, \beta_3\}$ also works if controlled in such a way that the edge parameters $\boldsymbol{\Psi} = (\ldots, \Psi_e, \ldots)^\mathsf{T}$ are changed independently, see Sec. B of [41].

For edge parametrization, we call the responses $d_{p_{e'}} j_e$ and $P_{ee'}$ local (nonlocal) if the perturbation edge e' does (does not) coincide with the observation edge e. In Sec. C of [41] we prove that the diagonal elements of $\mathbb{P}$ are bounded,

$$0 \leq P_{ee} \leq 1, \tag{15}$$

which implies the bounds for the local scaled responses

$$0 \leq \left(\frac{\partial j_e}{\partial p_e}\right)^{-1} \frac{d j_e}{d p_e} \leq 1. \tag{16}$$

This result extends a previous bounds obtained in Ref. [25] for specific parametrizations and perturbations of the rates.

Using the property of idempotent matrices $\mathrm{tr}\mathbb{P} = \mathrm{rk}\mathbb{P} = N_c$, we can further derive the following CRRs:

$$\sum_{e=1}^{N_e} \left(\frac{\partial j_e}{\partial p_e}\right)^{-1} \frac{d j_e}{d p_e} = N_c. \tag{17}$$

Since the lhs is the sum of local scaled responses that are bounded by Eq. (16), Eq. (17) show that if exactly N_c local sensitives are saturated, then the other ones must be zero. This will be illustrated in Fig. 3.

Unicyclic networks—We further restrict our theory to systems with a single cycle. Unicyclic systems play an
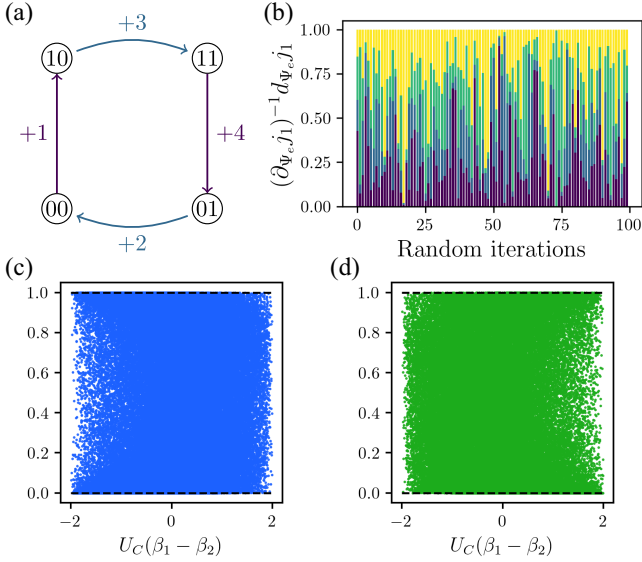
FIG. 2. (a) Unicyclic network obtained by removing the third reservoir from Fig. 1. (b) The heights of the purple, blue, green, and yellow bins correspond to the scaled responses of j_1 to perturbation of $\Psi_1, \ldots, \Psi_4$ for Γ_e, β_1, β_2 randomly and homogeneously distributed in $0 \leq \Gamma_e \leq 100$ and $0 \leq \beta_1, \beta_2 \leq 2$, with $U_C = 1$, $\mu_1 = \mu_2 = 1$. In (c), respectively, (d), $(T_1 d_{\epsilon_u} j_1 + |\partial_{\Psi_1} j_1|)/(|\partial_{\Psi_1} j_1| + |\partial_{\Psi_4} j_4|)$, respectively, $(T_2 d_{\epsilon_d} j_1 + |\partial_{\Psi_3} j_3|)/(|\partial_{\Psi_2} j_2| + |\partial_{\Psi_3} j_3|)$, bounded between 0 and 1.

important role in understanding molecular motors and metabolic networks; see, e.g., the dynein model in [49] and the biochemical switch in [28]. Choosing an edge orientation such that c consists only of $1s$ and $0s$ and using Eqs. (2) and (9) for the unicyclic system, we have $P_{ee'} = c_e B_{1e'}$ and $j_e = \mathcal{J} c_e$, where $\mathcal{J}$ is the flux and c_e are the elements of the single cycle c, that result in $P_{ee'} = c_e/c_{e'} P_{e'e'} = j_e/j_{e'} P_{e'e'}$ Using Eq. (14) and that if $j_e, j_{e'} \neq 0$ then $j_e = j_{e'}$, we find $P_{e'e'} = P_{ee'} = (\partial_{p_{e'}} j_{e'})^{-1} d_{p_e} j_e$ which results in the following bounds [see Eq. (15)]:

$$0 \leq \left(\frac{\partial j_{e'}}{\partial p_{e'}}\right)^{-1} \frac{d j_e}{d p_{e'}} \leq 1 \qquad (18)$$

for any combinations of the perturbing e' and observing e edges. In addition, the SRR (11) for the unicyclic network becomes

$$\sum_{e=1}^{N_e} \left(\frac{\partial j_e}{\partial p_e}\right)^{-1} \frac{d j_{e'}}{d p_e} = 1. \qquad (19)$$

Since scaled responses are non-negative and add up to one, the saturation of one automatically suppresses all the others.

Physical example: By removing the third reservoir (edge 5 and 6) and changing the orientation of the edges 2 and 4 in Fig. 1, the model becomes a four-state unicyclic

network, see Fig. 2(a). The histogram in Fig. 2(b) illustrates that the scaled responses to edge parameters Ψ are nonnegative and sum up to one as predicted by Eqs. (18) and (19). One also sees that they are typically shared between all edges, whereas when one tends to saturate, the other ones are suppressed. In Sec. D of [41] we derive the following tight bounds for the responses of any edge current j_e to the energy levels ϵ_u and ϵ_d: $-|\partial_{\Psi_1} j_1| \leq T_1 d_{\epsilon_u} j_e \leq |\partial_{\Psi_4} j_4|$ and $-|\partial_{\Psi_3} j_3| \leq T_2 d_{\epsilon_d} j_e \leq |\partial_{\Psi_2} j_2|$, which are illustrated for different values of the thermodynamic force $U_C(\beta_1 - \beta_2)$ in Figs. 2(c) and 2(d).

Multicycle systems—Since the elements of $\mathbb{C}$ can always be written using $\{0, 1\}$, the parametric dependence of the matrix $\mathbb{P}$ is defined by the $N_c N_e$ elements of the matrix $\mathbb{B}$ in Eq. (9), which satisfies $\mathbb{CBC} = \mathbb{C}$ due to Eq. (8). Matrix $\mathbb{C}$ is full column rank and $\mathbb{BC} = \mathbb{I}_c$ is the identity matrix of size N_c. Defining $\bar{\mathbb{C}}$ as the invertible submatrix of $\mathbb{C}$ and noting that it is always possible to define cycles such that $\bar{\mathbb{C}} = \mathbb{I}_c$,

$$\mathbb{BC} = \mathbb{B}\begin{pmatrix} \mathbb{I}_c \\ \tilde{\mathbb{C}} \end{pmatrix} = (\bar{\mathbb{B}}, \tilde{\mathbb{B}})\begin{pmatrix} \mathbb{I}_c \\ \tilde{\mathbb{C}} \end{pmatrix} = \mathbb{I}_c, \quad \bar{\mathbb{B}} = \mathbb{I}_c - \tilde{\mathbb{B}}\tilde{\mathbb{C}}, \qquad (20)$$

which reduces the number of unknown elements of $\mathbb{P}$ to $\#\text{var} = N_c N_e - N_c^2 = N_c(N - 1)$ elements of $\tilde{\mathbb{B}}$.

For edge parametrization, the fact that the scaled responses are bounded [Eq. (16)] can be used to find the set of bounded nonlocal responses. For edge currents, it is equivalent to finding nondiagonal elements $P_{ee'}$ that can be written in terms of only diagonal ones P_{ee} and thus be bounded. To do so, we define the number of independent diagonal elements as $\#\text{ide}$, which reduces the free variables of $\mathbb{P}$ to $\#\text{var} - \#\text{ide}$. Since there is always at least one constraint on diagonal elements because $\text{tr}\mathbb{P} = \text{rk}\mathbb{P}$, we have $\#\text{ide} \leq N_e - 1$. A greater number of constraints arise in systems with disjoint cycles (i.e., cycles that do not share edges), see Sec. E of [41] with an illustration for proof-reading networks [6]. All nondiagonal elements are bounded when

$$\#\text{var} - \#\text{ide} = (N_c - 1)(N - 2) + (N_e - 1 - \#\text{ide}) = 0, \qquad (21)$$

which is only possible if $\#\text{ide} = N_e - 1$, and thus if $N_c = 1$ (unicyclic models) or if $N = 2$ (two states models).

Beyond unicyclic and two-state models, only part of the possible responses are bounded by a linear combination of the local responses. To identify which ones, using Eqs. (9) and (20), we write

$$(\mathbb{I}_c - \tilde{\mathbb{B}}\,\tilde{\mathbb{C}})_{ee} = P_{ee}, \qquad e \leq N_c, \qquad (22a)$$

$$(\tilde{\mathbb{C}}\,\tilde{\mathbb{B}})_{ee} = P_{ee}, \qquad e > N_c. \qquad (22b)$$

This system of $\#\text{ide}$ equations allows us to express $\#\text{ide}$ elements $\{B_{\gamma e}^{\text{lin}}\}$ as a linear combination of the bounded
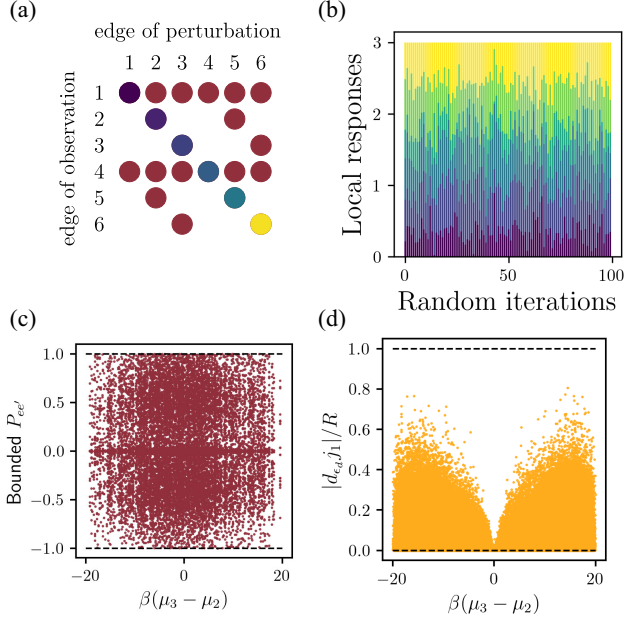
FIG. 3.   For the model in Fig. 1: (a) The disks indicate the 20 bounded $P_{ee'}$'s out of 36. (b) Validity of the CRR [Eq. (17)] with $N_c = 3$. The heights of the color bins (from black to yellow) correspond to P_{ee} for $e = 1, ..., 6$ and to randomly and homogeneously distributed $0 \leq \epsilon_u, \epsilon_d, U_C \leq 5$, $0 < \Gamma_e \leq 1000$ and $-10 \leq \mu_2, \mu_3 \leq 10$, with $T_i = 1$, $\mu_1 = 0$. (c) $P_{ee'}$ corresponding to the red disks in (a), as a function of the thermodynamic force $\beta(\mu_3 - \mu_2)$. (d) Physical responses $|d_{\epsilon_d} j_1|$ in units of $R = \sum_{e \neq 1,4} |\partial_{\Psi_e} j_e|$. Dashed lines denote our bounds.

diagonal elements $\{P_{ee}\}$. The other elements $\{B_{\gamma e}\} \backslash \{B_{\gamma e}^{\text{lin}}\}$ are not restricted by the bounds in Eq. (15). Thus, the elements $P_{ee'} = \sum_\gamma C_{e\gamma} B_{\gamma e'}$ are therefore bounded if they contain only terms from the set $\{B_{\gamma e}^{\text{lin}}\}$. This will be illustrated in Fig. 3.

Thermodynamic responses—The rates can be expressed in terms of their symmetric $v_e \equiv \ln\sqrt{W_{+e}W_{-e}} = v_{-e}$ and antisymmetric $w_e \equiv \ln\sqrt{W_{+e}/W_{-e}} = -w_{-e}$ parts as $W_{\pm e} = \exp(v_e \pm w_e)$. For the QDs of Fig. 1, $v_e = \ln\Gamma_e$ and $w_e = -\ln[1 + \exp(\Psi_e)]$. This decomposition is used in stochastic thermodynamics (i.e., for open systems undergoing transitions caused by thermal reservoirs) because the antisymmetric part defines the energetics of the system [46,50]:

$$\ln\frac{W_{+e}}{W_{-e}} = \sum_{i \in \mathcal{S}} E_i S_{ie} + \mathcal{F}_e, \quad \mathcal{F}_e = \sum_{\alpha \in \mathcal{R}} X_{e\alpha} f_\alpha. \quad (23)$$

The lhs of Eq. (23) is the entropy change in the reservoirs caused by a transition e. It can always be split, in the rhs, as a change in the Massieu potential E_i of the state i and as a nonconservative contribution $\mathcal{F}_e = -\mathcal{F}_{-e}$. The latter can be expressed, in Eq. (23), as a sum over a subset of reservoirs $\mathcal{R}$, where each term consists of an amount of conserved quantities exchanged with the reservoirs during

a transition e, $X_{e\alpha}$, multiplied by a conjugated (fundamental [46]) thermodynamic force, f_α made of differences of intensive fields of the reservoirs such as inverse temperatures or chemical potentials [46]. Using Eqs. (23) and (14), we find

$$d_{f_\alpha} j_e = \sum_{\rho \in \mathcal{E}} d_{f_\alpha} \mathcal{F}_\rho d_{\mathcal{F}_\rho} j_e = \sum_{\rho \in \mathcal{E}} X_{\rho\alpha} P_{e\rho} \partial_{\mathcal{F}_\rho} j_\rho, \quad (24)$$

which can be obtained analytically for known $\partial_{\mathcal{F}_\rho} j_\rho$. Since the (fundamental [46]) currents exchanged with the different reservoirs are the elements of the vector $\boldsymbol{I} = \mathbb{X}^{\mathsf{T}} j$, their response to the thermodynamic forces read

$$\mathbb{R}^I \equiv [d_{f_{\alpha'}} I_\alpha]_{\{\alpha, \alpha'\}} = \mathbb{X}^{\mathsf{T}} \mathbb{P} \mathbb{J}(\mathcal{F}) \mathbb{X} = \mathbb{X}^{\mathsf{T}} \mathbb{R}^j \mathbb{X}, \quad (25)$$

where $\alpha, \alpha' \in \mathcal{R}$ and $\mathbb{J}(\mathcal{F}) = \text{diag}(..., \partial_{\mathcal{F}_e} j_e, ...)$. Close to equilibrium, $\mathbb{R}^I$ reduces to the semipositive definite Onsager matrix (Sec. F of [41]). The lack of symmetry of $\mathbb{R}^I$ can thus be measured experimentally as $|R^I_{\alpha\alpha'} - R^I_{\alpha'\alpha}|$ and used to determine if the system is far from equilibrium.

Let us now assume that w_e is independent of v_e. This is relevant, for example, for Arrhenius-like rates [25], as well as for electron transfer rates in CMOS transistors [51] or single electron tunneling rates in the wide-band approximation [48]. Equation (23) shows that w_e depends only on the perturbation of the energy and forces, but does not depend on the perturbation of the kinetic parameters. Such kinetic v_e and energy (thermodynamic forces) w_e perturbations will be constrained by Eq. (11). Calculating the partial derivatives $\partial_{w_e} j_e = \tau_e$ and $\partial_{v_e} j_e = j_e$, we find $\phi_e = j_e/\tau_e$ (respectively, $\phi_e = 1$) for w_e (respectively, v_e), where $\tau_e \equiv W_e \pi_{s(+e)} + W_{-e} \pi_{s(-e)}$ is the edge traffic. Inserting ϕ_e into Eq. (11), we arrive at the symmetric and antisymmetric SRRs

$$\sum_e \frac{j_e}{\tau_e} d_{w_e} \boldsymbol{\pi} = \mathbf{0}, \qquad \sum_e d_{v_e} \boldsymbol{\pi} = \mathbf{0}, \quad (26a)$$

$$\sum_e \frac{j_e}{\tau_e} d_{w_e} \ln\boldsymbol{j} = \mathbf{1}, \qquad \sum_e d_{v_e} \ln\boldsymbol{j} = \mathbf{1}. \quad (26b)$$

We note that unlike the antisymmetric parametrization, the symmetric one is homogeneous $\boldsymbol{h} = (..., v_e, ...)^{\mathsf{T}}$ as the symmetric RSSs in Eq. (26) coincide with Eqs. (4) and (5).

Physical example: For the QDs in Fig. 1, we use Eq. (22) to find all the elements $P_{ee'}$ that are linear combinations of diagonal elements and are thus bounded, see Sec. G of [41] and Fig. 3(a). The 6 local scaled responses, P_{ee}, sum to $N_c = 3$ as predicted by the CRR [Eq. (17)], see Fig. 3(b). The nonlocal scaled responses can be negative, but those marked as disks in Fig. 3(a) are bounded as $-1 \leq P_{ee'} \leq 1$, see Eq. (G4) in [41] and Fig. 3(c). We use the properties of the matrix $\mathbb{P}$ to bound the responses of the current to physical parameters in Sec. H

of [41]. We find that $d_p j_\alpha = \sum_e P_{\alpha e} \partial_p \Psi_e$ for $\alpha = 1, 4$, where $-1 \leq P_{\alpha e} \leq 1$. We also find $|d_{\epsilon_d} j_\alpha| \leq R$, where $R = |\partial_{\Psi_2} j_2| + |\partial_{\Psi_3} j_3| + |\partial_{\Psi_5} j_5| + |\partial_{\Psi_6} j_6|$. This is illustrated numerically in Fig. 3(d) for different values of the thermodynamic force $\beta(\mu_3 - \mu_2)$, where we see that large responses arise far from equilibrium.

Future studies—Our approach provides powerful tools to identify networks that are highly sensitive or extremely resilient to perturbations. It is also ideally suited to study the responses of enzymatic changes (proofreading, sensing) in chemical reaction networks, in particular in conjunction with recently developed circuit theory [52]. Extending our approach to non-stationary response theory of Markov processes as in Refs. [35,36,53,54] is also an interesting perspective.

[1] X.-J. Zhang, H. Qian, and M. Qian, Phys. Rep. **510**, 1 (2012).

[2] H. Ge, M. Qian, and H. Qian, Phys. Rep. **510**, 87 (2012).

[3] J. A. Owen and J. M. Horowitz, Nat. Commun. **14**, 1280 (2023).

[4] A. Cornish-Bowden, *Fundamentals of Enzyme Kinetics* (John Wiley & Sons, New York, 2013).

[5] D. Fell and A. Cornish-Bowden, *Understanding the Control of Metabolism* (Portland Press, London, 1997), Vol. 2.

[6] A. Murugan, D. A. Huse, and S. Leibler, Phys. Rev. X **4**, 021016 (2014).

[7] N. Freitas, J.-C. Delvenne, and M. Esposito, Phys. Rev. X **11**, 031064 (2021).

[8] S. V. Moreira, P. Samuelsson, and P. P. Potts, Phys. Rev. Lett. **131**, 220405 (2023).

[9] J. Sohl-Dickstein, E. Weiss, N. Maheswaranathan, and S. Ganguli, in *International Conference on Machine Learning* (PMLR, Lille, France, 2015), pp. 2256–2265.

[10] R. Kubo, Rep. Prog. Phys. **29**, 255 (1966).

[11] C. C. Govern and P. R. ten Wolde, Phys. Rev. Lett. **113**, 258102 (2014).

[12] G. S. Agarwal, Z. Phys. A Hadrons Nucl. **252**, 25 (1972).

[13] U. Seifert and T. Speck, Europhys. Lett. **89**, 10007 (2010).

[14] J. Prost, J. F. Joanny, and J. M. R. Parrondo, Phys. Rev. Lett. **103**, 090601 (2009).

[15] B. Altaner, M. Polettini, and M. Esposito, Phys. Rev. Lett. **117**, 180601 (2016).

[16] M. Baiesi, C. Maes, and B. Wynants, Phys. Rev. Lett. **103**, 010602 (2009).

[17] M. Baiesi and C. Maes, New J. Phys. **15**, 013004 (2013).

[18] T. Hatano and S. I. Sasa, Phys. Rev. Lett. **86**, 3463 (2001).

[19] G. Falasco, T. Cossetto, E. Penocchio, and M. Esposito, New J. Phys. **21**, 073005 (2019).

[20] N. Shiraishi, Phys. Rev. Lett. **129**, 020602 (2022).

[21] A. Dechant and S.-i. Sasa, Proc. Natl. Acad. Sci. U.S.A. **117**, 6430 (2020).

[22] G. Szabó and G. Fath, Phys. Rep. **446**, 97 (2007).

[23] H.-M. Chun and J. M. Horowitz, J. Chem. Phys. **158**, 174115 (2023).

[24] Q. Gao, H.-M. Chun, and J. M. Horowitz, Europhys. Lett. **146**, 31001 (2024).

[25] T. Aslyamov and M. Esposito, Phys. Rev. Lett. **132**, 037101 (2024).

[26] E. De Giuli, arXiv:2308.10744.

[27] C. Floyd, A. R. Dinner, and S. Vaikuntanathan, arXiv:2404.03798.

[28] J. A. Owen, T. R. Gingrich, and J. M. Horowitz, Phys. Rev. X **10**, 011066 (2020).

[29] G. Fernandes Martins and J. M. Horowitz, Phys. Rev. E **108**, 044113 (2023).

[30] J. Schnakenberg, Rev. Mod. Phys. **48**, 571 (1976).

[31] N. G. Van Kampen, *Stochastic Processes in Physics and Chemistry* (Elsevier, New York, 1992), Vol. 1.

[32] J. Gunawardena, PLoS One **7**, e36321 (2012).

[33] S. G. M. Srinivas, F. Avanzini, and M. Esposito, Phys. Rev. E **109**, 064153 (2024).

[34] T. Aslyamov, F. Avanzini, E. Fodor, and M. Esposito, Phys. Rev. Lett. **131**, 138301 (2023).

[35] P. E. Harunari, S. D. Cengio, V. Lecomte, and M. Polettini, Phys. Rev. Lett. **133**, 047401 (2024).

[36] J. Zheng and Z. Lu, arXiv:2403.10952.

[37] R. Heinrich and T. A. Rapoport, Eur. J. Biochem. **42**, 89 (1974).

[38] H. Kacser, J. A. Burns, H. Kacser, and D. Fell, Biochem. Soc. Trans. **23**, 341 (1995).

[39] C. Reder, J. Theor. Biol. **135**, 175 (1988).

[40] R. Heinrich and S. Schuster, *The Regulation of Cellular Systems* (Springer Science & Business Media, New York, 2012).

[41] See Supplemental Material at http://link.aps.org/supplemental/10.1103/PhysRevLett.133.107103 for the derivation of Eq. (6) (Sec. A); discussion of the physical parameters (Sec. B); proof of Eq. (15) (Sec. C); discussion of physical perturbations in unicyclic networks (Sec. D); calculation of the number of independent diagonal elements (Sec. E); limits close to equilibrium (Sec. F); calculations of the bounded configurations (Sec. G); discussion of physical perturbations in multicyclic networks (Sec. H); which includes Refs. [6,25,42,43].

[42] S. R. de Groot and P. Mazur, *Non-Equilibrium Thermodynamics* (Dover, New York, 1984).

[43] D. Forastiere, R. Rao, and M. Esposito, New J. Phys. **24**, 083021 (2022).

[44] J. J. Brust, R. F. Marcia, and C. G. Petra, SIAM J. Matrix Anal. Appl. **41**, 852 (2020).

[45] P. Strasberg, G. Schaller, T. Brandes, and M. Esposito, Phys. Rev. Lett. **110**, 040601 (2013).

[46] R. Rao and M. Esposito, New J. Phys. **20**, 023007 (2018).

[47] P. E. Harunari, Phys. Rev. E **110**, 024122 (2024).

[48] R. Sánchez, P. Samuelsson, and P. P. Potts, Phys. Rev. Res. **1**, 033066 (2019).

[49] W. Hwang and C. Hyeon, J. Phys. Chem. Lett. **9**, 513 (2018).

[50] G. Falasco and M. Esposito, arXiv:2307.12406.

[51] A. Gopal, M. Esposito, and N. Freitas, Phys. Rev. B **106**, 155303 (2022).

[52] F. Avanzini, N. Freitas, and M. Esposito, Phys. Rev. X **13**, 021041 (2023).

[53] A. Y. Mitrophanov, J. Appl. Probab. **40**, 970 (2003).

[54] A. Y. Mitrophanov, J. Appl. Probab. **42**, 1003 (2005).